

Article

Removal of Metals by Biomass Derived Adsorbent in Its Granular and Powdered Forms: Adsorption Capacity and Kinetics Analysis

Ana Beatriz Soares Aguiar¹, Josiel Martins Costa^{2,*}, Gabriela Espirito Santos¹, Giselle Patrícia Sancinetti¹ and Renata Piacentini Rodriguez¹

¹ Laboratory of Anaerobic Biotechnology—Science and Technology Institute, Federal University of Alfenas (UNIFAL-MG), José Aurélio Vilela Road, BR 267, km 533, 11999, Poços de Caldas 37715-400, MG, Brazil

² School of Food Engineering (FEA), University of Campinas (UNICAMP), Campinas 13083-862, SP, Brazil

* Correspondence: josiel.martins.costa@gmail.com

Abstract: Among the various existing metals, zinc and copper are predominant metals in several effluents from industries such as electroplating, plastics production and mining. Technical methods have been applied in the treatment of effluents containing metals, including chemical removal, adsorption, ion exchange, membrane technologies and electrochemistry. However, it is necessary to develop technologies that minimize costs and increase treatment quality while reducing residual sludge generation. Adsorption using biological materials stands out for removing metals, a low-cost technique and high efficiency. Thus, this study evaluated metal adsorption using an adsorbent from granular and powdered anaerobic sludge, followed by a kinetic analysis, aiming at a new alternative for wastewater treatment. Evaluation of the copper and zinc adsorption process using granular and powdered biomass resulted in maximum removals of 72.9% and 62.7% for zinc, respectively, and 92.8% and 85.0% for copper, respectively. Analyzing the kinetic models, the pseudo-second-order model fitted the data better. Applying the kinetics of other studies in the literature for copper and zinc removal by other adsorbents, the pseudo-second-order model was the most representative model. In this context, kinetic modeling allowed the determination of the solute removal rate, estimating the adsorption mechanism.

Keywords: heavy metal; modeling; pseudo-second-order model; wastewater treatment



Citation: Aguiar, A.B.S.; Costa, J.M.; Santos, G.E.; Sancinetti, G.P.; Rodriguez, R.P. Removal of Metals by Biomass Derived Adsorbent in Its Granular and Powdered Forms: Adsorption Capacity and Kinetics Analysis. *Sustain. Chem.* **2022**, *3*, 535–550. <https://doi.org/10.3390/suschem3040033>

Academic Editor: Florent Allais

Received: 31 October 2022

Accepted: 30 November 2022

Published: 2 December 2022

Publisher's Note: MDPI stays neutral with regard to jurisdictional claims in published maps and institutional affiliations.



Copyright: © 2022 by the authors. Licensee MDPI, Basel, Switzerland. This article is an open access article distributed under the terms and conditions of the Creative Commons Attribution (CC BY) license (<https://creativecommons.org/licenses/by/4.0/>).

1. Introduction

Accelerated growth combined with poor management, especially in waste generation, brings severe environmental and public health challenges. Among the significant environmental impacts is an increase in concentration of metals in the soil and water resulting from human activities such as mining, metallurgy and agricultural production [1]. Metal ions are toxic components. Therefore, they cause environmental damage [2]. In addition, their presence in surface and groundwater has become an environmental concern due to their toxicity and tendency to bioaccumulate, especially when combined with accelerated industrial and economic development [3].

Zinc-containing effluents result from industrial activities such as electroplating, paint, battery, cosmetic, rubber, plastic, pharmaceutical production, and mine wastewater. High concentrations of this metal in the human body can cause disease emergence, skin irritation, and vomiting, among other effects [4]. Another relevant metal is copper, used in industrial activities such as metal finishing, electroplating, plastic production and corrosion. Copper is a toxic and harmful metal even at low concentrations. Therefore, effluents containing this metal must be treated before being discharged into the environment [5].

In Brazil, the National Environmental Council (CONAMA), established by the National Environmental Policy, regulates aspects of environmental licensing. The effluent discharge standards in Brazil state that the maximum concentrations are 5 mg L^{-1} for zinc and 1 mg L^{-1} for dissolved copper [6]. Therefore, the search for efficient and economical metal removal and recovery technologies has been the focus of research in recent years. Currently, the main forms of treatment of effluents containing metals are chemical precipitation, adsorption, ion exchange, membrane technologies and electrochemistry. However, there is a growing desire to develop technologies that offer a more attractive cost/benefit ratio with less waste sludge generation [7].

The biosorption technique, derived from the adsorption process, consists of the adhesion of contaminants, such as metals, on the surface or inside a solid material used as an adsorbent. The technique is a cost-effective and efficient alternative for removing various pollutants from wastewater and water [8,9]. In this way, the bioadsorbent is a biological matrix represented by components of microbial, plant, animal and derived products, resulting in a sustainable and economical process [10]. The biological matrix can be classified into active and inactive biomass. Inactive biomass is chemically more stable than active biomass, although the latter has more binding points for metallic adhesion and, therefore, greater interaction power [11]. However, when using active biomass, the system is susceptible to problems such as toxicity caused by metals and requires greater control over environmental conditions due to microorganisms [12].

In the process of metal biosorption, metal ions bind to functional groups of the biomass derived adsorbent (BDA), such as amine, sulfate, carboxyl, phosphate and hydroxyl groups [13]. However, variables such as pH, temperature, the particle size of the BDA and the equilibrium state of the medium can influence the process [10]. Several studies have analyzed the influence of process parameters on system efficiency [12,14,15]. The pH is one of the most important factors in adsorption since it interferes with the availability of binding sites and the activity of functional groups on the surface of the BDA. It modifies the adsorbent's active sites, making it necessary to use an optimal range that favors the adsorption process. Likewise, it interferes with the adsorption capacity of metal ions, influencing the protonation of binding sites and the degree of ionization.

The process is classified according to the metal ions' location at the end of the treatment. In intracellular biosorption, metals are adsorbed inside the cell membrane of the BDA. Cell surface biosorption presents the binding of metal ions to the cell surface of the BDA through physicochemical interactions. Finally, extracellular precipitation allows the assimilation of metal uptake between the cell surface and the aqueous medium [16]. The choice of BDA is essential to ensure the effective development of the system. It must be chosen considering the process's economy, efficiency and speed [14].

Many studies have evaluated the feasibility of different BDAs in metal biosorption systems, including biochar with sewage sludge to capture Cd^{2+} , Pb^{2+} and Zn^{2+} ions and other pollutants [17] and the use of sugarcane bagasse to remove Pb^{2+} , Cu^{2+} and Zn^{2+} [18]. Thus, the search for methods that increase the biosorption capacity of BDAs has been intensified through pre-treatments, such as physicochemical treatment, which consists of techniques capable of modifying the properties of the BDA [19]. The main physical surface modification methods are freezing, crushing, boiling/heating and drying. Chemical methods include polymerization, binding-site modification and washing. Physical methods are simpler and more economical, whereas chemical methods are more efficient in optimizing the biosorption capacity [16].

Adsorption kinetics allows understanding the process of removing a contaminant and obtaining the residence time of the adsorbate at the interface between the solid phase and the fluid medium. Therefore, it is defined as the solute removal rate. Furthermore, information about the adsorption mechanism and association of theoretical models with experimental behavior can be obtained. Thus, kinetic modeling is essential to guide biosorption studies since the equations and interpretation of the models help in determining

the solute removal rate, estimating the adsorption mechanism and sizing reactors and effluent treatment systems.

The kinetic models of the adsorption mechanism are classified into reaction models and diffusion models [20]. The reaction models can be pseudo-first-order, pseudo-second-order, or Elovich. However, they may not represent the experimental data, requiring other models, such as the Weber and Morris model (diffusion model). Diffusion models assume that intraparticle diffusion is the rate-limiting step of biosorption, and reaction models assume that the rate-limiting step of biosorption occurs due to chemisorption [21]. Therefore, this study evaluated metal adsorption systems (Cu^{2+} and Zn^{2+}) using granular and powdered anaerobic sludge as adsorbent. Kinetic analysis of the adsorption process considered the pseudo-first-order, pseudo-second-order, Elovich, and Weber and Morris model.

2. Materials and Methods

2.1. Biomass Derived Adsorbent and Adsorbate Solution

The BDA was a biological sludge from an anaerobic sludge blanket reactor used to treat effluents from poultry slaughterhouses (Aviculture Dacar, Tietê-SP, Brazil). Thermal and physical treatments were applied to modify the cell surface, inactivate the sludge, and increase its adsorption performance. First, the process removed excess water in the sludge using a commercial household sieve. Subsequently, the sludge was dried in an oven for 48 h at 100 °C. Next, the material was transferred to a commercial sieve, where the material retained in the sieve was called granular biomass, and the filtered particles were considered powdery biomass. Finally, the powdered biomass was macerated with a pestle to reduce the particle size. The mass of BDA used in the adsorption process was defined as a function of the determination of total solids (ST) and fixed and volatile total solids (FTS and VTS), according to the Standard Methods for Examination of Water and Wastewater-2540 Solids [22].

The adsorbate solution was prepared from salt and ZnCl_2 for a final zinc concentration of 14.5 mg L^{-1} ; the pH of the medium did not change, presenting a value of 5.29 ± 0.01 . Finally, the 10 mg L^{-1} copper solution was prepared using CuCl_2 . Again, the pH of the solution did not change, with a value equal to 4.66 ± 0.01 . The pH measurement was performed using a digital bench pH meter (Bel Engineering, PHS3BW).

2.2. Fourier Transform Infrared Spectroscopy Analysis

FTIR analyses were performed on an Agilent® model Cary 630 FTIR Spectrometer, in attenuated total reflectance mode with a sweep between 4000 and 500 cm^{-1} and resolution of 4 cm^{-1} .

2.3. Experimental Procedure

All the materials used in the experimental setup were immersed for 24 h in a solution of HNO_3 10% (*v/v*) and then washed with distilled water to protect from the removal of residual trace metals. Subsequently, the materials were sterilized in an autoclave at 121 °C for 30 min, as suggested by Mogensen et al. [23]. The tests were performed under conditions of complete asepsis. Antibiotic-type glass vials with a reaction volume of 100 mL were used. The vial was filled with 5 g L^{-1} of dry BDA (59.5 g SV L^{-1}) and subsequently autoclaved. Then, 80 mL of the copper or zinc solution was added to the flask containing the dry BDA. The reactors were closed with a butyl cap and metal seal. All experiments were performed in triplicate. The flasks were stored in a shaker incubator with constant orbital shaking (170 rpm), heating and a controlled temperature (30 °C). The kinetic analyses of adsorption were performed at different times: 0, 2, 4, 24, 48, and 72 h.

For analysis of the metal concentration in the liquid phase, samples were collected at regular intervals at the end of each adsorption period. First, a sterilized set of syringes and needles was used to remove the sample (18 mL), which was transferred to a Falcon tube, where 30 μL of an HNO_3 solution (10%) was added. Then, the samples were frozen for further analysis of the metal concentrations in the solution.

2.4. Determination of Metal Concentration

For each sample, the concentrations of Cu^{2+} and Zn^{2+} were analyzed. First, the copper and zinc adsorption test aliquots were centrifuged at 3500 rpm for 10 min and vacuum filtered for clarification. Then, at 24, 48, and 72 h in the copper samples, a solution of aqua regia ($\text{HCl} + \text{HNO}_3$) was added, and the samples were placed in a biodigester for 15 min at $150\text{ }^\circ\text{C}$; a longer contact time between the BDA and the copper solution produces a darker color in the samples. Finally, the Cu and Zn concentrations were determined by high-resolution continuous source atomic absorption spectrometry (model 300, Analytik Jena-HR CS-AAS).

2.5. Kinetic Modeling

The ability of BDA to remove Zn^{2+} and Cu^{2+} ions from the adsorption system was determined by the amount of metal adsorbed per mass of BDA over time. Equation (1) describes the adsorption capacity (q_t) at time t :

$$q_t = \frac{V(C_0 - C_t)}{m} \quad (1)$$

where q_t is the adsorbed amount of zinc or copper per mass of BDA (mg g^{-1}), V —solution volume (L), C_0 —initial concentration of metal ions in the solution (mg L^{-1}), C_t —concentration of metal ions in the solution at time t (mg L^{-1}), and m —dry mass of the BDA (g).

2.5.1. Pseudo-First-Order Model

Equation (2) expresses the pseudo-first-order model developed by Lagergren. It is used when the rate of adsorption to binding sites is proportional to the number of unoccupied sites in the BDA. Adsorption systems on solid surfaces immersed in a liquid solution containing a solute also follow this model. Its use is suitable for initial biosorption times, up to 20% solute adsorption. However, after this surface charge, there are changes in the solute concentration in the aqueous solution, and the number of active sites available for incorporation of the adsorbate decreases, making the model not very applicable [24].

$$\frac{dq_t}{dt} = k_1(q_e - q_t) \quad (2)$$

where k_1 —pseudo-first-order adsorption rate constant (min^{-1}), q_e and q_t —adsorbed quantities per gram of adsorbent biomass at equilibrium and at time t , respectively (mg g^{-1}).

By integrating Equation (2) and applying the following boundary conditions, $q_t = 0$ and $t = 0$, Equation (3) is obtained:

$$\ln(q_e - q_t) = \ln q_e - k_1 t \quad (3)$$

The pseudo-first-order adsorption rate constant can be obtained from the $\ln(q_e - q_t)$ versus t graph.

2.5.2. Pseudo-Second-Order Model

Equation (4) describes the pseudo-second-order model. It is used when the occupancy rate of the adsorbent sites is proportional to the square of the number of unoccupied sites [25]:

$$\frac{dq_t}{dt} = k_2(q_e - q_t)^2 \quad (4)$$

where k_2 —pseudo-second-order adsorption rate constant ($\text{g mg}^{-1} \text{min}^{-1}$), and q_e and q_t —adsorbed quantities per gram of adsorbent biomass at equilibrium and at time t , respectively (mg g^{-1}).

After integration and linearization, Equation (5) is obtained:

$$\frac{t}{q_t} = \frac{1}{k_2 q_e^2} + \frac{t}{q_e} \quad (5)$$

The intercept and slope of the t/q_t versus t curve give the pseudo-second-order adsorption rate constant and the amount adsorbed per gram of adsorbent biomass at equilibrium. The constant considers that chemisorption is the limiting step of the adsorption process. Therefore, the system depends on the adsorption capacity of the BDA related to the number of active sites available.

2.5.3. Weber and Morris Model

The adsorption rate-limiting mechanism is a step in the diffusion of molecules in the fluid into the pores. Therefore, the Weber and Morris model states that adsorption varies almost proportionally with half of the time power ($t^{0.5}$), as described by Equation (6).

$$q_t = K_d t^{0.5} + C \quad (6)$$

where q_t —amount of adsorbate adsorbed on the solid phase (mg g^{-1}) at time t (min), K_d —intraparticle diffusion coefficient ($\text{mg g}^{-1} \text{min}^{-1}$), and C —constant related to the diffusion resistance (mg g^{-1}).

The slope of the line and the intersection of the curve q_t versus $t^{0.5}$ provides the values of k_d and C . They can help interpret the process as the thickness of the boundary layer since the value of C is directly proportional to the layer effect limit in the adsorption system. The model describes that during the initial adsorption steps, the linear coefficient is zero, indicating that intrapore diffusion controls the adsorption process. However, for a non-zero linear coefficient, the film diffusion controls adoption, and the thickness of this boundary layer may be related to the linear coefficient value.

2.5.4. Elovich Model

The Elovich kinetic model, according to Equation (8), was initially described for the process of chemical adsorption of a gas on the surface of a solid material. However, this model also describes the adsorption processes of various substances in a liquid medium.

$$\frac{dq_t}{dt} = \alpha e^{-\beta q_t} \quad (7)$$

Moreover, the nonlinear equation derived from Equation (7) is described by Equation (8):

$$q_t = \frac{1}{\beta} \ln(1 + \alpha \beta t) \quad (8)$$

where α —initial adsorption rate ($\text{mg g}^{-1} \text{min}^{-1}$); β —adsorption constant (mg g^{-1}); and q_t —amount of adsorbed adsorbent per amount of adsorbent (mg g^{-1}) at time t (min).

Integrating Equation (8) and applying the following boundary conditions, $q_t = 0$ and $t = 0$, Equation (9) is obtained.

$$q = \frac{1}{\beta} \ln(\alpha \beta) + \frac{1}{\beta} \ln(t) \quad (9)$$

The curve q versus $\ln(t)$ provides the parameters α and β . The Elovich equation describes the chemical adsorption mechanism, representing the interaction between the adsorbent and the adsorbate as a chemical reaction (chemisorption) [26]. The Elovich model is accurate, fitting the kinetic data properly throughout almost the entire adsorption period, with errors only at the end of the process due to slow adsorption [27].

3. Results and Discussion

3.1. Removal of Metal Ions

Table 1 displays data on metal ion removal during zinc and copper adsorption by powdered and granular inactive anaerobic biomass.

Table 1. Adsorption capacity of Zn^{2+} and Cu^{2+} metal ions in the adsorption process.

Time (min)	Zinc ($mg\ g^{-1}$)		Copper ($mg\ g^{-1}$)	
	Granular	Powdered	Granular	Powdered
0	0.16 ± 0.06	0.39 ± 0.04	0.19 ± 0.15	0.41 ± 0.09
120	0.78 ± 0.02	1.03 ± 0.02	0.73 ± 0.01	0.78 ± 0.02
240	0.82 ± 0.03	1.07 ± 0.05	1.17 ± 0.01	0.88 ± 0.00
1440	1.47 ± 0.04	1.25 ± 0.02	1.61 ± 0.04	1.23 ± 0.00
2880	1.81 ± 0.02	1.58 ± 0.05	1.59 ± 0.00	1.47 ± 0.00
4320	1.83 ± 0.01	1.46 ± 0.01	1.59 ± 0.00	1.40 ± 0.01

The constant adsorbate concentration in the fluid medium or the insignificant amount of adsorbate removed determines the equilibrium of the adsorption process. For zinc adsorption systems, equilibrium occurred within 48 h. For copper, equilibrium was reached for granular biomass in 24 h and powdered biomass in 48 h. Figure 1 displays the amount of adsorbed ions (Zn^{2+} and Cu^{2+}) from the aqueous solution by the granular and powdered biomass.

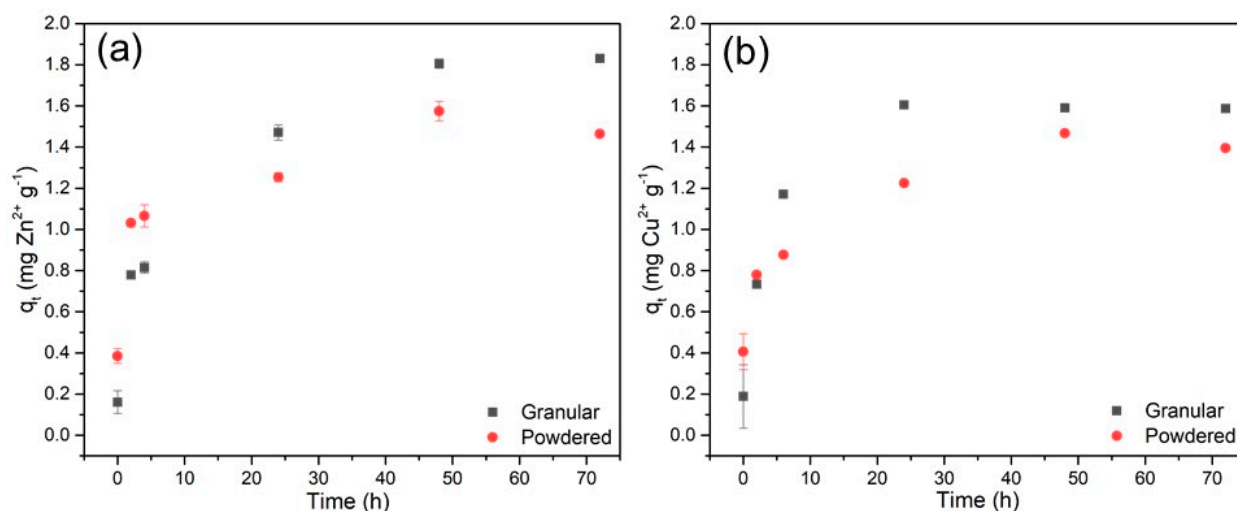


Figure 1. Adsorption curve of metallic ions by granular and powdered biomass: (a) Zn^{2+} ; (b) Cu^{2+} .

The adsorption process presents phases associated with the steps of adsorption kinetics. It depends on the initial transport of metal ions from the aqueous solution to the outer surface of the BDA. The ions diffuse to the surface of the pores. Then, they are adsorbed on the active sites within the pores, reaching equilibrium. The quantification of metal ions adsorbed by the granular biomass was superior to that of the powdered BDA, contrary to expectations since the powdered biomass presented a greater external surface area. For zinc removal, granular biomass reached a final removal of 72.9% and powder—58.3%. For copper, the removal for granular biomass was 91.8%, and for powder—80.9%. The performance efficiency of the adsorbent depends on its selectivity and affinity for the respective ion compared to competing ion, ionic properties and ion concentration. Likewise, adsorbent characteristics, metal ion properties and liquid medium characteristics are parameters that impact adsorbent performance [28,29]. In addition, the acidic property of the metal influences the adsorption of metals. A more acidic heavy metal reacts easily with a protonated site compared to a weaker acidic heavy metal. Different experimental

adsorption analyses indicate that the adsorbent affinity follows the order $\text{Cu} > \text{Zn}$ [30]. The significance test of the variables indicated that there was a significant difference ($p < 0.05$) for the adsorption time for both metals. The biomass granulometry was significant for the Cu^{2+} adsorption ($p < 0.05$). On the other hand, for Zn^{2+} adsorption, the significance test indicated $p = 0.48$ for biomass granulometry, showing no effect on adsorption.

Norton et al. [31] evaluated the removal of Zn^{2+} ions in aqueous solutions from the application of biosolids collected from an activated sludge system of an effluent treatment plant. Zinc removal occurred at different concentrations, including the concentration of 19.6 mg L^{-1} , a value close to that evaluated in this study. Equilibrium was reached after 5 h, with a maximum removal of 86.7%. In another study, Shanmugaprasanth and Sivakumar [32] evaluated a biosorption system using an oil cake derived from the extraction of biodiesel oil as a biosorbent. The ion removal efficiency ranged from 68.42% to 81.45% for different metal concentrations. Yang et al. [33] reported that a zinc ion biosorption system using dry activated sludge had removal efficiencies ranging from 17.6% to 89%.

Terry and Stone [34] studied a copper biosorption system from green algae species *Scenedesmus abundans*. The authors obtained a reduction in the copper concentration from 10 mg L^{-1} to 0.1 mg L^{-1} in 36 h. Pavasant et al. [35] investigated the sorption of Cu^{2+} by the dry green macroalgae *Caulerpa lentillifera*. The removal efficiency increased to a specific pH value, reaching a range in metal removal between 50% and 85%. Finally, Lacerda et al. [36] evaluated a copper biosorption system using the dead biomass of a filamentous fungus (*Penicillium ochrochloron*). The authors observed 75% removal of Cu^{2+} ions for a system with an initial copper concentration of 50 mg L^{-1} .

3.2. Characterization of the Biomass Composition

FTIR spectra were obtained for the granular biomass treated at 100°C , as shown in Figure 2.

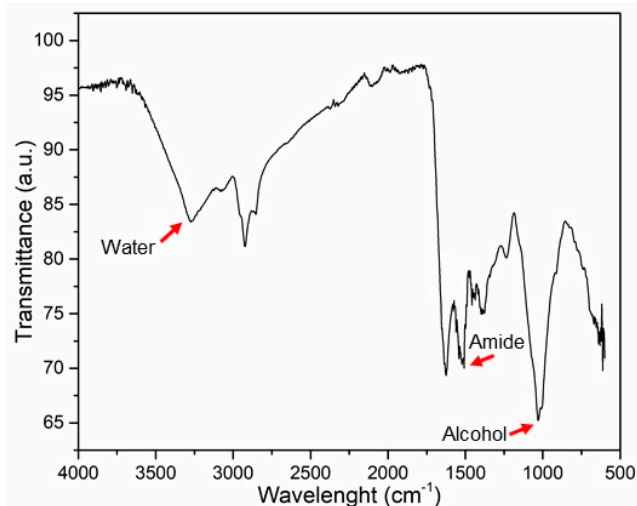


Figure 2. FTIR spectra of the granular biomass.

The band referring to water was observed at 3250 cm^{-1} . Likewise, methyl and methylene groups were identified at 2960 and 2925 cm^{-1} , respectively. Primary amides were observed at 1634 and 1627 cm^{-1} . At 1540 cm^{-1} two bands referring to secondary amide groups were observed. C–O bond groups referring to carbohydrates and alcohols are assigned in the region between 1250 and 1000 cm^{-1} . Thus, polysaccharides and cellulose carbohydrates were assigned to bands at 1034 and 1024 cm^{-1} . Furthermore, bands attributed to –OH groups of mineral compounds were identified between 1070 and 1000 cm^{-1} . Yang et al. [33] reported a similar FTIR spectra for Zn^{2+} biosorption using dry activated sludge with a particle size of $250 \mu\text{m}$ as BDA. The authors observed a decrease in the adsorption intensity of the amide group at 1637 and 1543 cm^{-1} , demonstrating that this group played an important role in zinc binding. The vibration of –C–O–C and –OH from

polysaccharides resulted in a band at 1036 cm^{-1} . In addition, the $-\text{OH}$ group was involved in zinc binding.

3.3. Kinetic Analyses

3.3.1. Pseudo-First-Order Model

Table 2 displays the parameters of the pseudo-first-order kinetic model based on Equations (1) and (2).

Table 2. Parameters of the pseudo-first-order kinetic model.

Metal	Parameters ¹	Granular Biomass	Powdered Biomass
Zinc	$q_e\text{ exp (mg g}^{-1}\text{)}$	1.81	1.58
	$q_e\text{ adj (mg g}^{-1}\text{)}$	1.35	0.71
	$k_1\text{ (min}^{-1}\text{)}$	0.00	0.00
	R^2	0.95	0.87
Copper	$q_e\text{ exp (mg g}^{-1}\text{)}$	1.61	1.47
	$q_e\text{ adj (mg g}^{-1}\text{)}$	0.83	0.76
	$k_1\text{ (min}^{-1}\text{)}$	0.00	0.00
	R^2	0.90	0.95

¹ $q_e\text{ exp}$: experimental value of the adsorbed quantity at equilibrium; $q_e\text{ adj}$: adjusted value of the adsorbed quantity at equilibrium.

The linear regression coefficient (R^2) and the similarity between the experimental and adjusted value of the adsorbed amount of metal per adsorbent mass at equilibrium allowed evaluation of the representativeness of the model. For the zinc system, the granular biomass data had a good fit to the pseudo-first-order model ($R^2 = 0.95$), with values close to $q_e\text{ exp}$ and $q_e\text{ adj}$. For the copper system, the powder biomass also indicated a good correlation with the model ($R^2 = 0.95$); however, with a greater difference between the values of $q_e\text{ exp}$ and $q_e\text{ adj}$.

High values of R^2 for the pseudo-first-order model in the metal biosorption systems have been reported in the literature [20,37–39]. Furthermore, the adsorption data fitted to a pseudo-first-order model indicate that a chemical phenomenon may limit the sorption kinetics since the chemical reactions and/or the diffusion of the liquid film in the boundary layer is responsible for the resistance to the mass transfer [40].

3.3.2. Pseudo-Second-Order Model

Table 3 displays the parameters of the pseudo-second-order kinetic model based on Equations (4) and (5).

Table 3. Parameters of the pseudo-second-order kinetic model.

Metal	Parameters	Granular Biomass	Powdered Biomass
Zinc	$q_e\text{ exp (mg g}^{-1}\text{)}$	1.81	1.58
	$q_e\text{ adj (mg g}^{-1}\text{)}$	1.90	1.51
	$k_2\text{ (g mg}^{-1}\text{ min}^{-1}\text{)}$	0.00	0.01
	R^2	0.99	0.99
Copper	$q_e\text{ exp (mg g}^{-1}\text{)}$	1.61	1.47
	$q_e\text{ adj (mg g}^{-1}\text{)}$	1.62	1.44
	$k_2\text{ (g mg}^{-1}\text{ min}^{-1}\text{)}$	0.01	0.01
	R^2	1.00	1.00

Data from both systems using powdered and granulated biomass fit well with the pseudo-second-order model, demonstrating high linear regression coefficients ($R^2 \geq 0.993$). For all conditions, the amount of metal adsorbed per mass of adsorbent in the experimental and adjusted equilibrium were close. According to Tan and Hameed [41], pseudo-first

and pseudo-second-order models are commonly applied to adsorption systems. However, the pseudo-first-order model generally presents data with less adjustability than the pseudo-second-order model due to mathematical factors during linearization since the random errors in the values of q_e are less expressive in the pseudo-second-order model [42]. Furthermore, these models are more descriptive than predictive due to the ease of curve fitting [41]. Several authors have reported the representativeness of the model in metal biosorption systems [43–45]. The systems point out that chemical sorption is the binding mechanism. The bond between the metal ions and the biosorbent occurs through an exchange of ions or covalent bonds [46].

3.3.3. Weber and Morris Model

Table 4 displays the parameters of the Weber and Morris kinetic model. The parameter C is related to the thickness of the boundary layer formed on the surface of the adsorbent particle. As it increases, the limiting effect of the layer is also enhanced.

Table 4. Parameters of the Weber and Morris kinetic model.

Metal	Parameters	Granular Biomass	Powdered Biomass
Zinc	K_d ($\text{mg g}^{-1} \text{min}^{-1}$)	0.02	0.01
	C (mg g^{-1})	0.38	0.69
	R^2	0.99	0.78
Copper	K_d ($\text{mg g}^{-1} \text{min}^{-1}$)	0.02	0.02
	C (mg g^{-1})	0.55	0.56
	R^2	0.77	0.91

The granular biomass ($R^2 = 0.99$) fits better for the zinc adsorption systems than the powdered biomass. In contrast, the powdered biomass ($R^2 = 0.91$) presented a better representation of the model with copper than the granular biomass. Studies have reported that the Weber and Morris model adjusted to metal biosorption with high values for the linear regression coefficient [25,37]. In most adsorption systems, the model presents multiple control mechanisms, in which the initial step consists of adsorption on the surface of the adsorbent. Subsequently, intraparticle diffusion becomes the process control mechanism, and in the third stage, the system tends to approach equilibrium [41].

3.3.4. Elovich Model

Table 5 displays the parameters α and β obtained by the Elovich model. The first is related to the initial rate of sorption, and the second to the size of the binding surface and the activation energy for chemisorption [47].

Table 5. Parameters of the Elovich kinetic model.

Metal	Parameters	Granular Biomass	Powdered Biomass
Zinc	α ($\text{mg g}^{-1} \text{min}^{-1}$)	0.02	1.27
	β (mg g^{-1})	3.08	7.01
	R^2	1.00	0.87
Copper	α ($\text{mg g}^{-1} \text{min}^{-1}$)	0.09	0.09
	β (mg g^{-1})	4.38	5.18
	R^2	0.87	0.97

The Elovich kinetics for zinc and granular biomass showed a good correlation ($R^2 = 1.00$). For copper, the powdered biomass indicated an $R^2 = 0.97$. Studies have reported this model for metal adsorption systems [26,48]. The adsorption system adjusted to the Elovich model indicates that the sorption tends to be controlled by chemisorption. The interaction between the biosorbent and the adsorbate occurs through a chemical bond [47].

3.4. Evaluation of Zn and Cu Adsorption Systems and Application of Kinetic Modeling

A broader kinetic study of zinc and copper adsorption processes considered data from several previous studies. The kinetic study of biosorption systems seeks to identify the time required to reach adsorption equilibrium and evaluate how the system responds to different parameters such as pH, temperature, sorbate concentration and biosorption concentration. Therefore, kinetic modeling was performed in the experimental system (S0). It evaluated the binding rate of metal ions on the surface of the BDA, being a process control step and probable binding mechanism.

3.4.1. Zinc Adsorption Systems

Zinc system 1 (S1-Zn), published by Melčáková and Růžovič [49], analyzed the performance of the filamentous green seaweed (*Spirogyra* sp.) and parts (root, stem and leaves) of a plant (*Reynoutria japonica*) in the biosorption process of an aqueous solution of zinc with a Zn^{2+} concentration of 10 mg L^{-1} . Zinc system 2 (S2-Zn) developed by Rodrigues et al. [50] evaluated the potential of using water lettuce (*Pistia stratiotes*) dry biomass for zinc biosorption, and the biomass performance was analyzed by varying the initial metal concentration. Finally, zinc system 3 (S3-Zn), published by Norton et al. [31], evaluated the potential of applying dry biosolids to remove Zn^{2+} ions from aqueous solutions. The BDA was collected from the activated sludge system of a wastewater treatment plant. Figure 3 exhibits the adsorption curves of the Zn^{2+} ion for the three evaluated systems.

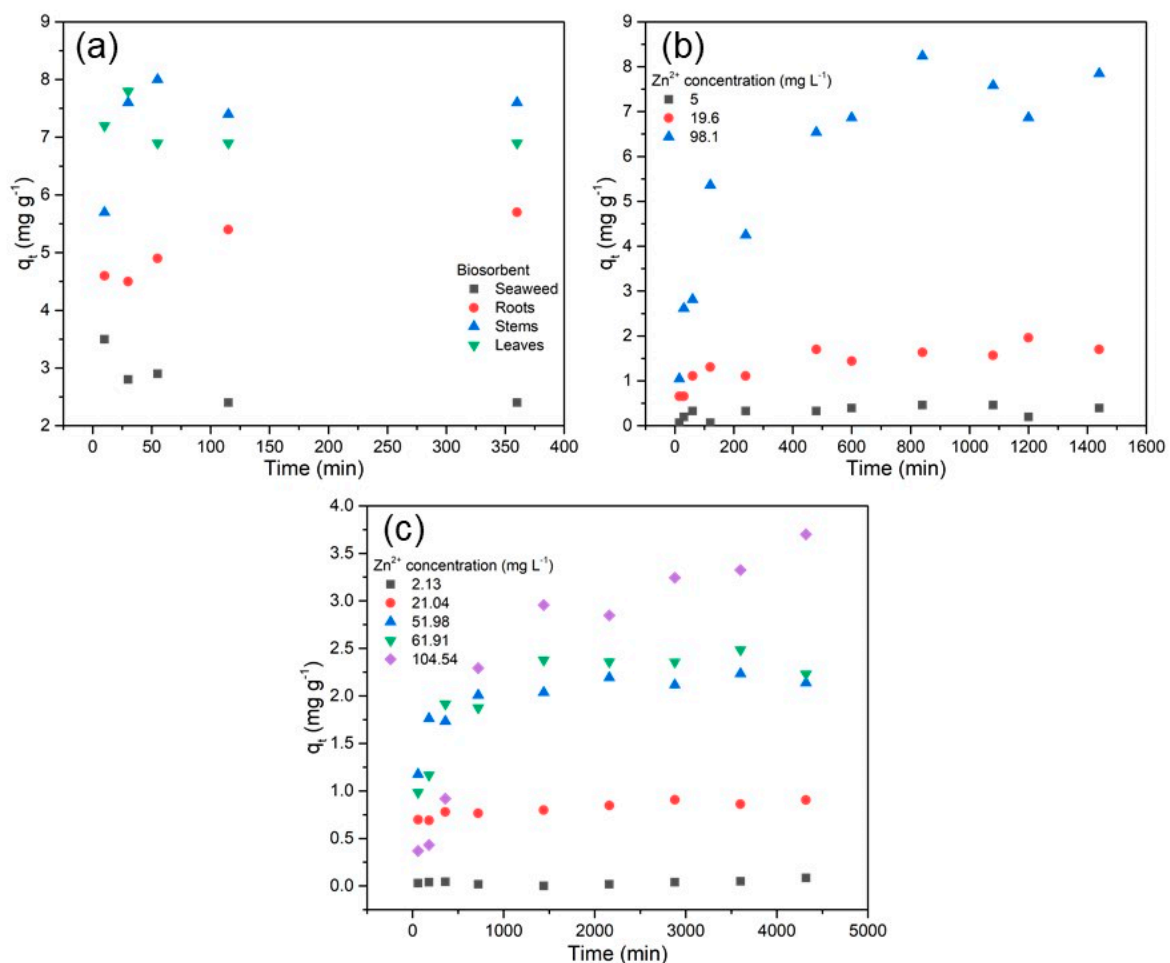


Figure 3. Adsorption curves of the Zn^{2+} ion for the systems: (a) S1-Zn—with different biosorbents [49]; (b) S2-Zn—with different initial concentrations of zinc [50]; (c) S3-Zn—with different initial concentrations of zinc [31].

The S1-Zn system (Table S1) reached equilibrium at different times for each biosorbent. Equilibrium was reached in approximately 10 min ($q_e = 3.5 \text{ mg g}^{-1}$)—green algae, 115 min—roots ($q_e = 5.4 \text{ mg g}^{-1}$) and 30 min—stems ($q_e = 7.6 \text{ mg g}^{-1}$) and leaves ($q_e = 7.8 \text{ mg g}^{-1}$). The stem of the plant *Reynoutria japonica* reached the maximum removal of Zn^{2+} ions of 80%, followed by the leaves (78%) and roots (57%). Seaweed *Spirogyra* sp. showed a maximum zinc removal rate of 17.5%.

For the S2-Zn system (Table S2), the adsorption capacity curve revealed that the samples with higher concentrations of zinc had a greater amount of adsorbed zinc per mass of biosorbent. The water lettuce dry biomass reached equilibrium at different times, according to the initial zinc concentration. For lower concentrations, equilibrium was reached in 6 h ($q_e = 0.045 \text{ mg g}^{-1}$), for median concentrations it occurred in 36 h ($q_e = 0.846, 2.192, \text{ and } 2.358 \text{ mg g}^{-1}$ for concentrations of 21.04, 51.98 and 61.91 mg L^{-1} , respectively), and at higher concentrations –72 h ($q_e = 3.701 \text{ mg g}^{-1}$). Furthermore, the removals varied according to the initial zinc concentration, following the ascending order of concentration with maximum removals of 79.3%, 86.1%, 85.9%, 80.3% and 70.8%.

The S3-Zn system (Table S3) reached equilibrium with a period of 4 h for the initial zinc concentration of 2 mg L^{-1} ($q_e = 0.327 \text{ mg g}^{-1}$), 8 h– 5 mg L^{-1} ($q_e = 1700 \text{ mg g}^{-1}$) and 24 h– 98.1 mg L^{-1} ($q_e = 7.846 \text{ mg g}^{-1}$). As observed in the previous study, the adsorption capacity was higher for higher initial concentrations of zinc. The maximum removals in ascending order of the initial Zn concentration were 91.5%, 86.7%, and 84%.

3.4.2. Copper Adsorption Systems

Copper system 1 (S1-Cu) investigated by Peng et al. [51] analyzed the efficiency of Cu^{2+} biosorption from an aqueous solution of ($\text{CuSO}_4 \cdot 5 \text{ H}_2\text{O}$) by immobilizing the fungus *Saccharomyces cerevisiae* (active cells) on the surface of chitosan-coated magnetic nanoparticles from an aqueous solution. Copper system 2 (S2-Cu) was described by Ianis et al. [52]. The authors analyzed the biosorption of an aqueous copper solution with a concentration of 100 mg L^{-1} by the fungus *Penicillium cyclopium* (active cells). Finally, copper system 3 (S3-Cu) was studied by Khormaei et al. [53]. The authors investigated the biosorption of copper by sour orange residues. The copper metal concentration during the biosorption process was 150 mg L^{-1} . Figure 4 exhibits the adsorption curves of the Cu^{2+} ion for the three evaluated systems.

The S1-Cu system (Table S4) indicated the high adsorption capacity of copper by the fungus *Saccharomyces cerevisiae* during the initial 20 min. Equilibrium was reached in 60 min ($q_e = 131 \text{ mg g}^{-1}$). The maximum copper removal by the fungal biomass was 66.5%. For the S2-Cu system (Table S5), the biomass rapidly adsorbed copper ions by the biomass in the first five minutes at both biosorbent concentrations. However, the biosorption started to stabilize in 25 min. It reached equilibrium in 60 min, with $q_e = 57.49 \text{ mg g}^{-1}$ for the biosorbent concentration of 0.9915 g L^{-1} and $q_e = 20.42 \text{ mg g}^{-1}$ for the biosorbent concentration of 3.9660 g L^{-1} . For high concentrations of biosorbent, the biosorption capacity decreases as diffusional limitations may occur. The mass transfer rate slows down and begins to limit the overall reaction rate [52]. The maximum copper removal by the fungal biomass of *Penicillium cyclopium* was 57%, with a biosorbent concentration of 0.9915 g L^{-1} and 3.9660 g L^{-1} – 81%. Therefore, increasing the concentration of the biosorbent resulted in the greater removal of metal ions.

For the S3-Cu system (Table S6), both biosorbent particle sizes rapidly biosorbed copper ions by orange residues within the first few minutes of analysis. Equilibrium times were different for each particle size: particles from 0.15 to 0.35 mm took 20 min ($q_e = 13.59 \text{ mg g}^{-1}$), while from 0.7 to 1.0 mm required 80 min ($q_e = 13.21 \text{ mg g}^{-1}$). The difference in equilibrium times is related to the high agitation speed (300 rpm) to overcome the diffusion resistance of the film resulting from intraparticle diffusion [53]. The removal of copper ions for the biosorbent with granulometry between 0.15 and 0.35 mm indicated a maximum value of 90.63%, and the particles of 0.7–1.0 mm were slightly

smaller at approximately 88.08%. The removal efficiency was higher for smaller sizes of biosorbent particles.

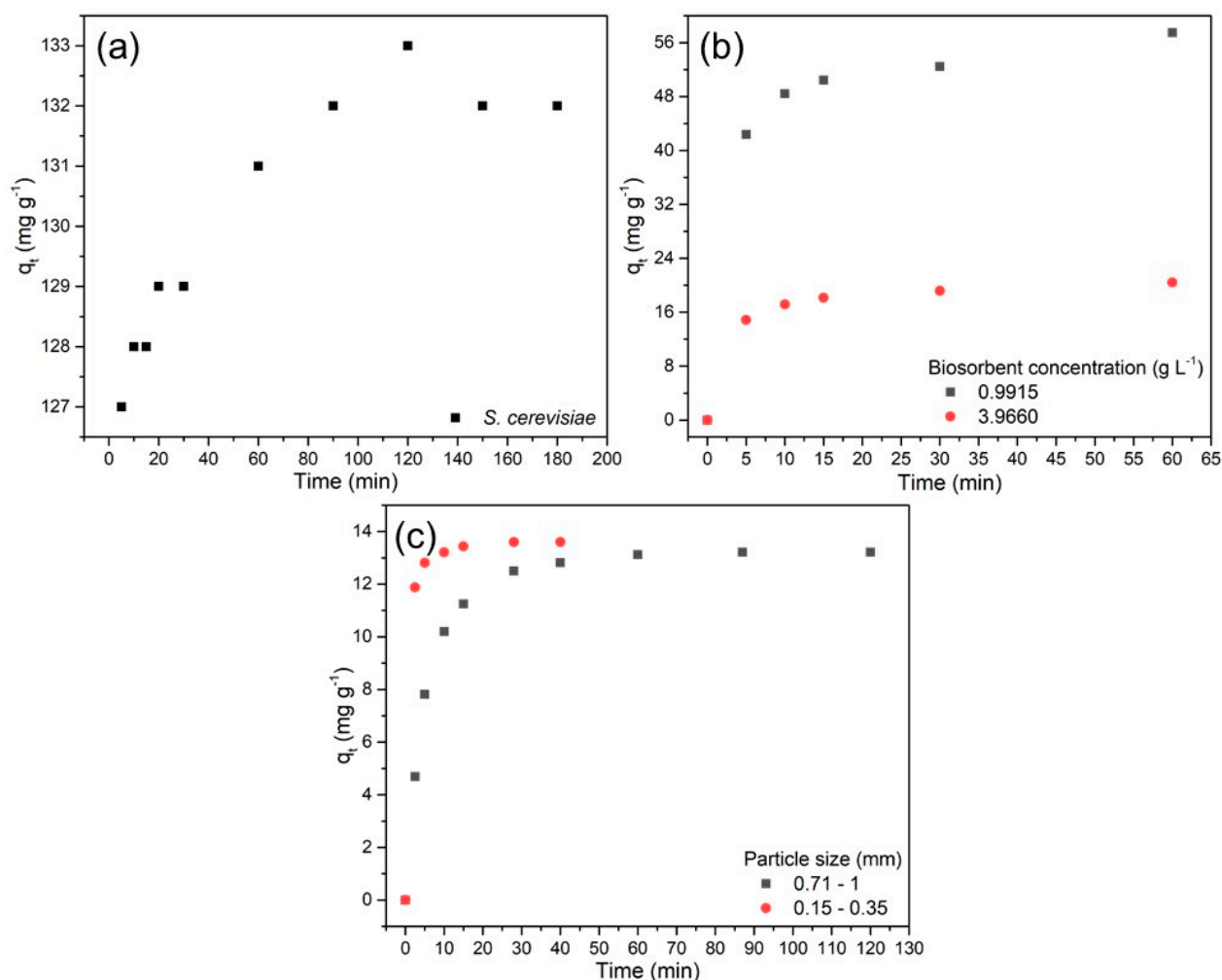


Figure 4. Adsorption curve of the Cu²⁺ ion for the systems: (a) S1-Cu—with *Saccharomyces cerevisiae* [51]; (b) S2-Cu—with different concentrations of biosorbent [52]; and (c) S3-Cu—with different biomass particle sizes [53].

3.4.3. Representativeness of the Pseudo-Second-Order Model in Metal Adsorption Systems

In addition to the experimental system, kinetic modeling of the zinc and copper systems was performed for the studies discussed above, considering the four kinetic models. Tables 6 and 7 show that the pseudo-second-order model indicated a more representative fit. Data for the adjustments considering the other models are available in the supplementary material.

As illustrated in Table 6, most systems showed high values for R². Only the systems that operated with a low initial concentration of zinc resulted in data that did not fit the model well, according to the S2-Zn and S3-Zn systems with different biosorbents. For all copper adsorption systems shown in Table 7, the R² value was 1.00, demonstrating the full fit of the experimental data to the model. The experimental and adjusted adsorption capacity was similar for all adsorbent materials.

The adsorption system data fitted to the pseudo-second-order model suggest that the interaction between the system components occurred through an exchange of electrons between the adsorbate (metal ions) and the adsorbent through the chemisorption process [54]. The data also showed a good fit to the Elovich model, where the limiting mechanism of the

process occurs due to chemical reactions. Therefore, zinc and copper adsorption are mainly limited by chemisorption mechanisms.

Table 6. Pseudo-second-order model parameters for zinc systems: S0-Zn, S1-Zn, S2-Zn and S3-Zn.

Data	Parameters	Granular Biomass	Powdered Biomass			
Experimental System (S0-Zn)	q_e exp (mg g ⁻¹)	1.81	1.58			
	q_e adj (mg g ⁻¹)	1.90	1.51			
	k_2 (g mg ⁻¹ min ⁻¹)	0.00	0.01			
	R^2	0.99	0.99			
System 1 (S1-Zn)		Green seaweed	Plant			
			Root	Stem	Leaf	
	q_e exp (mg g ⁻¹)	3.50	5.40	7.60	7.80	
	q_e adj (mg g ⁻¹)	2.36	5.80	7.62	6.87	
	k_2 (g mg ⁻¹ min ⁻¹)	-0.08	0.02	0.13	-0.12	
	R^2	1.00	1.00	1.00	1.00	
System 2 (S2-Zn)		Water lettuce dry biomass				
		2.13	21.04	51.98	61.91	104.54
			(mg Zn ²⁺ L ⁻¹)			
	q_e exp (mg g ⁻¹)	0.05	0.85	2.19	2.36	3.70
	q_e adj (mg g ⁻¹)	0.06	0.90	2.20	2.41	4.53
k_2 (g mg ⁻¹ min ⁻¹)	0.02	0.01	0.01	0.00	0.00	
	R^2	0.45	1.00	1.00	0.99	0.95
System 3 (S3-Zn)		Activated sludge system biomass				
		2.0	5.0	98.1		
			(mg Zn ²⁺ L ⁻¹)			
	q_e exp (mg g ⁻¹)	0.33	1.70	7.85		
	q_e adj (mg g ⁻¹)	0.35	1.80	8.18		
k_2 (g mg ⁻¹ min ⁻¹)	0.03	0.01	0.00			
	R^2	0.69	0.98	0.98		

Table 7. Pseudo-second-order model parameters for copper systems: S0-Cu, S1-Cu, S2-Cu, and S3-Cu.

Data	Parameters	Granular Biomass	Powdered Biomass
Experimental System (S0-Cu)	q_e exp (mg g ⁻¹)	1.61	1.47
	q_e adj (mg g ⁻¹)	1.62	1.44
	k_2 (g mg ⁻¹ min ⁻¹)	0.01	0.01
	R^2	1.00	1.00
System 1 (S1-Cu)		Fungus biomass—<i>Saccharomyces cerevisiae</i>	
	q_e exp (mg g ⁻¹)	131	
	q_e adj (mg g ⁻¹)	133.33	
	k_2 (g mg ⁻¹ min ⁻¹)	0.02	
	R^2	1	
System 2 (S2-Cu)		Fungus biomass—<i>Penicillium cyclopium</i>	
		0.9915	3.966
		(g L ⁻¹)	
	q_e exp (mg g ⁻¹)	57.49	20.42
q_e adj (mg g ⁻¹)	59.52	21.14	
k_2 (g mg ⁻¹ min ⁻¹)	0.01	0.02	
	R^2	1.00	1.00

Table 7. Cont.

Data	Parameters	Granular Biomass	Powdered Biomass
		Sour orange residue biomass	
System 3 (S3-Cu)		0.15–0.35	0.7–1.0
		(mm)	
	q_e exp (mg g ⁻¹)	13.59	13.21
	q_e adj (mg g ⁻¹)	13.68	1.62
	k_2 (g mg ⁻¹ min ⁻¹)	0.23	0.01
	R ²	1.00	1.00

4. Conclusions

The experimental system of adsorption of Zn²⁺ and Cu²⁺ ions by granular and powdered biomass proved efficient. The adsorption reached maximum removals of 72.9% (granular) and 62.7% (powder) for zinc, and 92.8% (granular) and 85.0% (powder) for copper. The evaluation of the kinetic models through the linear regression coefficient indicated that the pseudo-second-order model presented a high capacity for adjustment to the experimental data for the zinc and copper adsorption systems. Thus, as the kinetic model was based on chemical reactions, the adsorption rate-limiting step occurred due to chemisorption. In addition, the adsorption allowed the regeneration of the BDA and the possibility of recovering the metal. Therefore, investment in studies involving the kinetic analysis of the process becomes valid since the studies assist in development of projects and more efficient responses to the treatment of effluents. In addition, these actions contribute to the 6th Sustainable Development Goal, reducing pollution and improving water quality.

Supplementary Materials: The following supporting information can be downloaded at: <https://www.mdpi.com/article/10.3390/suschem3040033/s1>, Table S1: Parameters of the kinetic models for the S1-Zn system; Table S2: Parameters of the kinetic models for the S2-Zn system; Table S3: Parameters of the kinetic models for the S3-Zn system; Table S4: Parameters of the kinetic models for the S1-Cu system; Table S5: Parameters of the kinetic models for the S2-Cu system; Table S6: Parameters of the kinetic models for the S3-Cu system.

Author Contributions: Conceptualization, R.P.R.; methodology, A.B.S.A.; software, A.B.S.A.; validation, A.B.S.A. and G.E.S.; formal analysis, J.M.C., G.P.S. and R.P.R.; investigation, A.B.S.A. and G.E.S.; resources, R.P.R.; data curation, A.B.S.A. and G.E.S.; writing—original draft preparation, A.B.S.A.; writing—review and editing, J.M.C., G.P.S. and R.P.R.; visualization, R.P.R.; supervision, R.P.R.; project administration, R.P.R.; funding acquisition, R.P.R. All authors have read and agreed to the published version of the manuscript.

Funding: This research was funded by Coordenação de Aperfeiçoamento de Pessoal de Nível Superior—CAPES (finance code 001).

Institutional Review Board Statement: Not applicable.

Informed Consent Statement: Not applicable.

Data Availability Statement: The data presented in this study are available in supplementary material.

Conflicts of Interest: The authors declare no conflict of interest.

References

- Burakov, A.E.; Galunin, E.V.; Burakova, I.V.; Kucherova, A.E.; Agarwal, S.; Tkachev, A.G.; Gupta, V.K. Adsorption of heavy metals on conventional and nanostructured materials for wastewater treatment purposes: A review. *Ecotoxicol. Environ. Saf.* **2018**, *148*, 702–712. [[CrossRef](#)] [[PubMed](#)]
- Abdi, O.; Kazemi, M. A review study of biosorption of heavy metals and comparison between different biosorbents. *J. Mater. Environ. Sci.* **2015**, *6*, 1386–1399.
- Sulaymon, A. Biosorption of Heavy Metals: A Review. *J. Chem. Sci. Technol.* **2014**, *3*, 74–102.

4. Sen, T.K.; Gomez, D. Adsorption of zinc (Zn^{2+}) from aqueous solution on natural bentonite. *Desalination* **2011**, *267*, 286–294. [[CrossRef](#)]
5. Al-Saydeh, S.A.; El-Naas, M.H.; Zaidi, S.J. Copper removal from industrial wastewater: A comprehensive review. *J. Ind. Eng. Chem.* **2017**, *56*, 35–44. [[CrossRef](#)]
6. CONAMA. National Council for the Environment-Ministry of the Environment, In: Resolution number 430 of May 13, 2011. In Provides for the Conditions and Standards for Effluent Discharge, Complements and Amends Resolution Number 357 of March 17, 2005; Brasilia, Brazil. 2011. Available online: <https://www.braziliannr.com/brazilian-environmental-legislation/conama-resolution-43011/> (accessed on 30 October 2022).
7. Pagnanelli, F.; Cruz Viggi, C.; Toro, L. Isolation and quantification of cadmium removal mechanisms in batch reactors inoculated by sulphate reducing bacteria: Biosorption versus bioprecipitation. *Bioresour. Technol.* **2010**, *101*, 2981–2987. [[CrossRef](#)]
8. Liakos, E.V.; Rekos, K.; Giannakoudakis, D.A.; Mitropoulos, A.C.; Fu, J.; Kyzas, G.Z. Activated Porous Carbon Derived from Tea and Plane Tree Leaves Biomass for the Removal of Pharmaceutical Compounds from Wastewaters. *Antibiotics* **2021**, *10*, 65. [[CrossRef](#)]
9. Giannakoudakis, D.A.; Hosseini-Bandegharaei, A.; Tsafrakidou, P.; Triantafyllidis, K.S.; Kornaros, M.; Anastopoulos, I. Aloe vera waste biomass-based adsorbents for the removal of aquatic pollutants: A review. *J. Environ. Manag.* **2018**, *227*, 354–364. [[CrossRef](#)]
10. Michalak, I.; Chojnacka, K.; Witek-Krowiak, A. State of the Art for the Biosorption Process—A Review. *Appl. Biochem. Biotechnol.* **2013**, *170*, 1389–1416. [[CrossRef](#)]
11. Chang, J.-S.; Law, R.; Chang, C.-C. Biosorption of lead, copper and cadmium by biomass of *Pseudomonas aeruginosa* PU21. *Water Res.* **1997**, *31*, 1651–1658. [[CrossRef](#)]
12. Utgikar, V.; Chen, B.-Y.; Tabak, H.H.; Bishop, D.F.; Govind, R. Treatment of acid mine drainage: I. Equilibrium biosorption of zinc and copper on non-viable activated sludge. *Int. Biodeter. Biodegr.* **2000**, *46*, 19–28. [[CrossRef](#)]
13. He, J.; Chen, J.P. A comprehensive review on biosorption of heavy metals by algal biomass: Materials, performances, chemistry, and modeling simulation tools. *Bioresour. Technol.* **2014**, *160*, 67–78. [[CrossRef](#)] [[PubMed](#)]
14. Hadiani, M.R.; Darani, K.K.; Rahimifard, N.; Younesi, H. Biosorption of low concentration levels of Lead (II) and Cadmium (II) from aqueous solution by *Saccharomyces cerevisiae*: Response surface methodology. *Biocatal. Agric. Biotechnol.* **2018**, *15*, 25–34. [[CrossRef](#)]
15. Yu, B.; Zhang, Y.; Shukla, A.; Shukla, S.S.; Dorris, K.L. The removal of heavy metal from aqueous solutions by sawdust adsorption — removal of copper. *J. Hazard. Mater.* **2000**, *80*, 33–42. [[CrossRef](#)]
16. Freitas, G.R.; Silva, M.G.C.; Vieira, M.G.A. Biosorption technology for removal of toxic metals: A review of commercial biosorbents and patents. *Environ. Sci. Pollut. Res.* **2019**, *26*, 19097–19118. [[CrossRef](#)]
17. Bogusz, A.; Oleszczuk, P.; Dobrowolski, R. Adsorption and desorption of heavy metals by the sewage sludge and biochar-amended soil. *Environ. Geochem. Health* **2019**, *41*, 1663–1674. [[CrossRef](#)]
18. Wang, F.; Pan, Y.; Cai, P.; Guo, T.; Xiao, H. Single and binary adsorption of heavy metal ions from aqueous solutions using sugarcane cellulose-based adsorbent. *Bioresour. Technol.* **2017**, *241*, 482–490. [[CrossRef](#)]
19. Zeraatkar, A.K.; Ahmadzadeh, H.; Talebi, A.F.; Moheimani, N.R.; McHenry, M.P. Potential use of algae for heavy metal bioremediation, a critical review. *J. Environ. Manag.* **2016**, *181*, 817–831. [[CrossRef](#)]
20. Al-Degs, Y.S.; El-Barghouthi, M.I.; Issa, A.A.; Khraisheh, M.A.; Walker, G.M. Sorption of Zn(II), Pb(II), and Co(II) using natural sorbents: Equilibrium and kinetic studies. *Water Res.* **2006**, *40*, 2645–2658. [[CrossRef](#)]
21. Liu, Y.; Liu, Y.-J. Biosorption isotherms, kinetics and thermodynamics. *Sep. Purif. Technol.* **2008**, *61*, 229–242. [[CrossRef](#)]
22. Rice, E.W.; Baird, R.B.; Eaton, A.D. *Standard Methods for the Examination for Water and Wastewater*, 23rd ed.; American Public Health Association: Washington DC, USA, 2017.
23. Mogensen, A.S.; Haagensen, F.; Ahring, B.K. Anaerobic degradation of linear alkylbenzene sulfonate. *Environ. Toxicol. Chem.* **2003**, *22*, 706–711. [[CrossRef](#)] [[PubMed](#)]
24. Shek, T.-H.; Ma, A.; Lee, V.K.C.; McKay, G. Kinetics of zinc ions removal from effluents using ion exchange resin. *Chem. Eng. J.* **2009**, *146*, 63–70. [[CrossRef](#)]
25. Kumar, D.; Gaur, J.P. Chemical reaction- and particle diffusion-based kinetic modeling of metal biosorption by a *Phormidium* sp.-dominated cyanobacterial mat. *Bioresour. Technol.* **2011**, *102*, 633–640. [[CrossRef](#)] [[PubMed](#)]
26. Wu, F.-C.; Tseng, R.-L.; Juang, R.-S. Characteristics of Elovich equation used for the analysis of adsorption kinetics in dye-chitosan systems. *Chem. Eng. J.* **2009**, *150*, 366–373. [[CrossRef](#)]
27. Gundry, P.M.; Tompkins, F.C. Chemisorption of gases on metals. *Chem. Soc. Rev.* **1960**, *14*, 257–291. [[CrossRef](#)]
28. Esposito, A.; Pagnanelli, F.; Vegliò, F. pH-related equilibria models for biosorption in single metal systems. *Chem. Eng. Sci.* **2002**, *57*, 307–313. [[CrossRef](#)]
29. Aksu, Z.; Açikel, Ü.; Kabasakal, E.; Tezer, S. Equilibrium modelling of individual and simultaneous biosorption of chromium(VI) and nickel(II) onto dried activated sludge. *Water Res.* **2002**, *36*, 3063–3073. [[CrossRef](#)]
30. Pagnanelli, F.; Esposito, A.; Toro, L.; Vegliò, F. Metal speciation and pH effect on Pb, Cu, Zn and Cd biosorption onto *Sphaerotilus natans*: Langmuir-type empirical model. *Water Res.* **2003**, *37*, 627–633. [[CrossRef](#)]
31. Norton, L.; Baskaran, K.; McKenzie, T. Biosorption of zinc from aqueous solutions using biosolids. *Adv. Environ. Res.* **2004**, *8*, 629–635. [[CrossRef](#)]

32. Shanmugaprasanth, M.; Sivakumar, V. Batch and fixed-bed column studies for biosorption of Zn(II) ions onto pongamia oil cake (*Pongamia pinnata*) from biodiesel oil extraction. *J. Environ. Manag.* **2015**, *164*, 161–170. [[CrossRef](#)]
33. Yang, C.; Wang, J.; Lei, M.; Xie, G.; Zeng, G.; Luo, S. Biosorption of zinc(II) from aqueous solution by dried activated sludge. *J. Environ. Sci.* **2010**, *22*, 675–680. [[CrossRef](#)] [[PubMed](#)]
34. Terry, P.A.; Stone, W. Biosorption of cadmium and copper contaminated water by *Scenedesmus abundans*. *Chemosphere* **2002**, *47*, 249–255. [[CrossRef](#)] [[PubMed](#)]
35. Pavasant, P.; Apiratikul, R.; Sungkhum, V.; Suthiparinyanont, P.; Wattanachira, S.; Marhaba, T.F. Biosorption of Cu²⁺, Cd²⁺, Pb²⁺, and Zn²⁺ using dried marine green macroalga *Caulerpa lentillifera*. *Bioresour. Technol.* **2006**, *97*, 2321–2329. [[CrossRef](#)] [[PubMed](#)]
36. Lacerda, E.C.M.; Passos Galluzzi Baltazar, M.; Reis, T.A.; Nascimento, C.A.O.; Côrrea, B.; Gimenes, L.J. Copper biosorption from an aqueous solution by the dead biomass of *Penicillium ochrochloron*. *Environ. Monit. Assess.* **2019**, *191*, 247. [[CrossRef](#)] [[PubMed](#)]
37. Gupta, S.; Kumar, D.; Gaur, J.P. Kinetic and isotherm modeling of lead(II) sorption onto some waste plant materials. *Chem. Eng. J.* **2009**, *148*, 226–233. [[CrossRef](#)]
38. Singh, A.; Kumar, D.; Gaur, J.P. Removal of Cu(II) and Pb(II) by *Pithophora oedogonia*: Sorption, desorption and repeated use of the biomass. *J. Hazard. Mater.* **2008**, *152*, 1011–1019. [[CrossRef](#)]
39. Vilar, V.J.P.; Botelho, C.M.S.; Boaventura, R.A.R. Equilibrium and kinetic modelling of Cd(II) biosorption by algae *Gelidium* and agar extraction algal waste. *Water Res.* **2006**, *40*, 291–302. [[CrossRef](#)]
40. Ho, Y.S.; Ng, J.C.Y.; McKay, G. Kinetics of pollutant sorption by biosorbents: Review. *Sep. Purif. Rev.* **2000**, *29*, 189–232. [[CrossRef](#)]
41. Tan, K.L.; Hameed, B.H. Insight into the adsorption kinetics models for the removal of contaminants from aqueous solutions. *J. Taiwan Inst. Chem. Eng.* **2017**, *74*, 25–48. [[CrossRef](#)]
42. Plazinski, W.; Rudzinski, W.; Plazinska, A. Theoretical models of sorption kinetics including a surface reaction mechanism: A review. *Adv. Colloid Interface Sci.* **2009**, *152*, 2–13. [[CrossRef](#)]
43. Calero, M.; Blázquez, G.; Martín-Lara, M.A. Kinetic Modeling of the Biosorption of Lead(II) from Aqueous Solutions by Solid Waste Resulting from the Olive Oil Production. *J. Chem. Eng. Data* **2011**, *56*, 3053–3060. [[CrossRef](#)]
44. Sağ, Y.; Aktay, Y. Kinetic studies on sorption of Cr(VI) and Cu(II) ions by chitin, chitosan and *Rhizopus arrhizus*. *Biochem. Eng. J.* **2002**, *12*, 143–153. [[CrossRef](#)]
45. Vilar, V.J.P.; Botelho, C.M.S.; Boaventura, R.A.R. Chromium and zinc uptake by algae *Gelidium* and agar extraction algal waste: Kinetics and equilibrium. *J. Hazard. Mater.* **2007**, *149*, 643–649. [[CrossRef](#)] [[PubMed](#)]
46. Malamis, S.; Katsou, E. A review on zinc and nickel adsorption on natural and modified zeolite, bentonite and vermiculite: Examination of process parameters, kinetics and isotherms. *J. Hazard. Mater.* **2013**, *252–253*, 428–461. [[CrossRef](#)] [[PubMed](#)]
47. Elkady, M.F.; Ibrahim, A.M.; El-Latif, M.M.A. Assessment of the adsorption kinetics, equilibrium and thermodynamic for the potential removal of reactive red dye using eggshell biocomposite beads. *Desalination* **2011**, *278*, 412–423. [[CrossRef](#)]
48. Juang, R.-S.; Chen, M.-L. Application of the Elovich Equation to the Kinetics of Metal Sorption with Solvent-Impregnated Resins. *Ind. Eng. Chem. Res.* **1997**, *36*, 813–820. [[CrossRef](#)]
49. Melčáková, I.; Ružovič, T. Biosorption of zinc from aqueous solution using algae and plant biomass. *Nova Biotechnol. Chim.* **2010**, *1*, 33–43. [[CrossRef](#)]
50. Rodrigues, A.C.D.; Amaral Sobrinho, N.M.B.; Santos, F.S.; Santos, A.M.; Pereira, A.C.C.; Lima, E.S.A. Biosorption of Toxic Metals by Water Lettuce (*Pistia stratiotes*) Biomass. *Water Air Soil Pollut.* **2017**, *228*, 156. [[CrossRef](#)]
51. Peng, Q.; Liu, Y.; Zeng, G.; Xu, W.; Yang, C.; Zhang, J. Biosorption of copper(II) by immobilizing *Saccharomyces cerevisiae* on the surface of chitosan-coated magnetic nanoparticles from aqueous solution. *J. Hazard. Mater.* **2010**, *177*, 676–682. [[CrossRef](#)]
52. Ianis, M.; Tsekova, K.; Vasileva, S. Copper Biosorption by *Penicillium Cyclopium*: Equilibrium and Modelling Study. *Biotechnol. Biotechnol. Equip.* **2006**, *20*, 195–201. [[CrossRef](#)]
53. Khormaei, M.; Nasernejad, B.; Edrisi, M.; Eslamzadeh, T. Copper biosorption from aqueous solutions by sour orange residue. *J. Hazard. Mater.* **2007**, *149*, 269–274. [[CrossRef](#)] [[PubMed](#)]
54. Sillanpää, M.; Ncibi, M.C.; Matilainen, A.; Vepsäläinen, M. Removal of natural organic matter in drinking water treatment by coagulation: A comprehensive review. *Chemosphere* **2018**, *190*, 54–71. [[CrossRef](#)] [[PubMed](#)]